First published May 5, 2010; doi:10.1152/jn.00790.2009.

Neural Modulation by Binocular Disparity Greatest in Human Dorsal Visual Stream

Loredana Minini,[1] Andrew J. Parker,[1] and Holly Bridge[2]

[1]*Department of Physiology, Anatomy and Genetics and* [2]*Centre for Functional Magnetic Resonance Imaging of the Brain, Department of Clinical Neurology, John Radcliffe Hospital, University of Oxford, Oxford, United Kingdom*

Submitted 25 August 2009; accepted in final form 30 April 2010

Minini L, Parker AJ, Bridge H. Neural modulation by binocular disparity greatest in human dorsal visual stream. *J Neurophysiol* 104: 169–178, 2010. First published May 5, 2010; doi:10.1152/jn.00790.2009. Although cortical activation to binocular disparity can be demonstrated throughout occipital and parietal cortices, the relative contributions to depth perception made by different human cortical areas have not been established. To investigate whether different regions are optimized for specific disparity ranges, we have measured the responses of occipital and parietal areas to different magnitudes of binocular disparity. Using stimuli consisting of sinusoidal depth modulations, we measured cortical activation when the stimuli were located at pedestal disparities of 0, 0.1, 0.35, and 0.7° from fixation. Across all areas, occipital and parietal, there was an increase in BOLD signal with increasing pedestal disparity, compared with a plane at zero disparity. However, the greatest modulation of response by the different pedestals was found in the dorsal visual areas and the parietal areas. These differences contrast with the response to the zero disparity plane, compared with fixation, which is greatest in the early visual areas, smaller in the ventral and dorsal visual areas, and absent in parietal areas. Using the simultaneously acquired psychophysical data we also measured a greater response to correct than to incorrect trials, an effect that increased with rising pedestal disparity and was greatest in dorsal visual and parietal areas. These results illustrate that the dorsal stream, along both its occipital and parietal branches, can reliably discriminate a large range of disparities.

INTRODUCTION

The role of the dorsal and ventral visual streams in processing and exploiting disparity information has been the subject of considerable attention recently (Chandrasekaran et al. 2007; Neri 2005; Neri et al. 2004; Parker 2007). Neurophysiological studies in macaque monkeys have shown the presence of neurons selective for binocular disparity throughout the visual cortex and into the parietal lobe (for reviews, see Cumming and DeAngelis 2001; Parker 2007). Comparisons between early, dorsal, and ventral visual areas have measured the extent to which the disparity response of individual neurons reflects the animal's perception. Primary visual cortex (V1) appears to perform the initial stages of disparity processing, although its neuronal responses do not match perceptual performance in several ways (Cumming and Parker 1997, 1999, 2000). However, the responses of some ventral areas are better matched to the perceptual experience, particularly in V4 and inferotemporal cortex (IT; Janssen et al. 1999, 2003; Tanabe et al. 2004; Umeda et al. 2007). In comparison, evidence about the role of the dorsal stream in stereopsis is more ambiguous. There is strong evidence that the dorsal visual area V5/MT is involved in some stereoscopic visual tasks but not others. For example, V5/MT neurons show choice-related activity with several types of stereoscopic depth judgment (Bradley et al. 1998; Dodd et al. 2001; Uka and DeAngelis 2004, 2006). Furthermore, electrical microstimulation implies a causally significant role in certain depth discriminations. On the other hand, V5/MT neurons lack sensitivity to fine disparity in stereoacuity tasks (Uka and DeAngelis 2006) and these neurons do not appear to have solved the correspondence problem (Krug et al. 2004).

Despite these varied results from the dorsal stream, data from human functional magnetic resonance imaging (fMRI) studies of depth perception have consistently shown the strongest activity in dorsal areas, particularly V3A, V7, and forward into parietal regions (Backus et al. 2001; Georgieva et al. 2009; Tsao et al. 2003).

One basic issue that has not been addressed is the range of disparities to which different visual areas are maximally sensitive. To investigate this point, we used a paradigm in which pedestal disparities of different sizes were added to the stimulus. It has been shown psychophysically that adding a pedestal disparity to a stimulus increases thresholds for detecting changes in disparity (Schumer and Julesz 1984). The corresponding effects on level and pattern of cortical activation, however, have not been investigated.

In this study, we set our subjects the task of discriminating stereoscopic disparity while we simultaneously measured their cortical activations using fMRI. Based on neurophysiological findings (Uka and DeAngelis 2006), we predicted a greater sensitivity to large disparities in dorsal relative to early and ventrolateral regions. Since the stimulus is a sinusoidal modulation of disparity, there will always be some small disparities present, even at the largest pedestal disparity. We would thus not necessarily expect to see a decrease in response in early and ventral areas with increasing pedestal, but rather a plateau in the response in that the additional, larger disparities add little to the response. The stereoscopic task not only focuses spatial attention on the stimuli but also ensures that subjects are responding consistently to the stereoscopic aspects of the stimulus. Psychophysical performance in this task indicates that our paradigm has brought both spatial and featural attention under tight experimental control. Surprisingly, perhaps, we found an increase in blood oxygenation level dependent (BOLD) activity with increasing pedestal disparity across all areas when contrasted with a zero disparity flat plane. The greatest modulation induced by the pedestal was found in dorsal visual and parietal regions. Although the trend of increasing BOLD activation with increasing pedestal disparity

Address for reprint requests and other correspondence: L. Minini, Department of Physiology, Anatomy and Genetics, University of Oxford, Parks Road, Oxford OX1 3PT, UK (E-mail: lori.minini@dpag.ox.ac.uk).

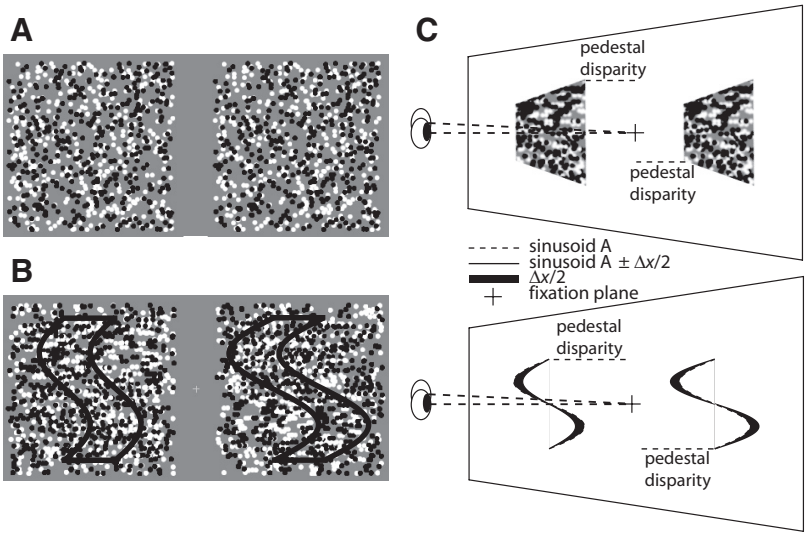

FIG. 1. *A*: fusible version of one of the 2 sinusoids in the display. *B*: the stimuli as shown in the scanner with a schematic drawing of the 2 sinusoids superimposed. The 2 stereograms were surrounded by a midgray background. *C*, *top*: schematic diagram showing the symmetrical arrangement of the stereograms around the fixation plane. *Bottom*: schematic diagram of the stimuli illustrating how depth was modulated by pedestal disparity, the sinusoidal amplitude, and disparity (Δx).

was present in ventrolateral areas, there were no significant differences with magnitude of pedestal disparity. This is consistent with Preston et al. (2008) who showed that the lateral occipital (LO) region is not modulated by disparity magnitude.

In contrast to the response to disparity modulation, the response magnitude to the zero disparity plane compared with fixation is greatest in early visual areas, smaller in both dorsal and ventral areas, and negligible in parietal regions. These results suggest that the ability of the dorsal and parietal regions to discriminate coarse disparities is considerably greater than that of the ventrolateral regions.

METHODS

Subjects

Four subjects (two male, aged 25–40 yr) participated in the experiment. They all had normal or corrected-to-normal self-reported visual acuity, stereo vision ≤120 arcsec. (TNO Stereo Test, Laméris, Utrecht, The Netherlands), and gave informed consent in accordance with the Oxfordshire Research Ethics Committee (05/Q1605/143).

Stimuli

Stimuli consisted of two 8 × 8° dynamic random-dot stereograms (RDSs) each containing 400 black (3.7 cd·m^{-2}) and white (173.7 cd·m^{-2}) antialiased dots (0.25° diameter) displayed on a midgray background (58.8 cd·m^{-2}). The centers of the two stereograms were horizontally aligned and located at 5° on either side of a central fixation cross (0.3° in size). The positions of the dots forming the RDS were dynamically updated to new randomly chosen locations at 12.5 Hz, while keeping the binocular disparities of the display constant. Each square envelope consisted of a surround zero disparity region and a 6.4 × 6.4° central region that could have a horizontal disparity of 0, 0.1, 0.35, or 0.7° (hereafter, "pedestal" disparity). Subpixel disparity resolution was obtained with antialiasing techniques. Laterally offsetting the central region generated gaps in the dot distribution that could have acted as monocular cues and were therefore filled with uncorrelated dots.

In each trial, the two stereograms were presented at the same pedestal disparity. However, to prevent systematic convergence of the eyes away from the plane of fixation, one stereogram was assigned a crossed pedestal disparity and the other stereogram an uncrossed pedestal disparity. The crossed/uncrossed direction of the depth displacement of each stereogram was controlled by a random function.

The depth of each plane was further modulated by adding one cycle of a vertical sinusoid (0.156 cycles/deg) whose amplitude was initially set at 0.20°. This was increased in the sinusoid on one side of the fixation plane and decreased in the sinusoid on the other side so that Δx was the resulting difference in amplitude between the two sinusoids. Specifically, $\Delta x/2$ was added to the amplitude of one sinusoid and subtracted from the amplitude of the other sinusoid in the pair. An example of the stimuli and schematic diagrams of the depth profiles are illustrated in Fig. 1. Figure 1*B* shows the stimuli as seen by the subjects in the scanner, with the addition of a schematic drawing of the two sinusoids to aid viewing.

The task of the subjects was to indicate which sinusoid had the greater amplitude in depth. This task ensured that the subjects were attending and responding to the depth information of both sinusoidal profiles in the two regions of the visual field.

To control for the possibility that a systematic increase in difficulty across pedestals could have confounded the results, we used Δx values that resulted in a correct performance of ≥75% at all pedestals. These values were determined empirically outside the scanner and are shown in Table 1. A pseudorandom function was used to assign Δx increments and decrements to the two RDSs and the two sinusoids were always presented in-phase. Cortical activation to the four disparity pedestals was assessed relative to a baseline condition that consisted of the two RDS patterns, with no disparity added, that is, zero disparity flat planes of dots.

Additional stimuli were created for two control conditions. The first controlled for the possibility that any effect of disparity across visual areas in the main experiment was due to different sensitivities to the zero disparity plane used as the baseline. We examined this by measuring the response to the zero disparity baseline relative to a fixation-only stimulus that consisted of the fixation cross presented on the midgray background. A second and larger set of stimuli was constructed to control for the possibility that systematic differences in the distribution of uncorrelated dots in the four pedestal conditions could have generated the pattern of results. As described earlier, the

TABLE 1. Δx *range used in the different pedestal disparities*

Pedestal Disparity	Δx Range; Step
0	−0.09 to 0.09; 0.03
0.1	−0.15 to 0.15; 0.05
0.35	−0.24 to 0.24; 0.08
0.7	−0.27 to 0.27; 0.09

All measurements are in degrees of visual angle.

gaps generated by the disparities and filled with uncorrelated dots necessarily varied in size across pedestals. The four pedestal conditions in these control (hereafter, "uncorrelated") stimuli were equivalent to the pedestals used in the main experiment for the pattern of uncorrelated dots, but they had identical disparities (i.e., correlated dots specifying the pedestal, sinusoid amplitude, and Δx) that were set as for the 0° pedestal in the main stimulus set. All the other stimulus parameters were as described earlier.

Functional data collection and psychophysics

All MRI images were acquired with a 3T whole-body TIM Trio scanner (Siemens, Erlangen, Germany) and a 12-channel receive-only head coil. Echo planar images (EPIs) consisted of 30 2.5-mm slices acquired coronally with an in-plane resolution of 2.2 × 2.2 mm (time to echo [TE] = 30 ms; repetition time [TR] = 2,000 ms; matrix = 64 × 64). The occipito-temporo-parietal region scanned with these parameters was approximately as excised by the mediolateral cut shown on the inflated hemisphere (Fig. 2, *top center*). Psychophysical and fMRI data were collected simultaneously in a block design across 10 runs distributed across two sessions. Each run gathered 210 volumes continuously and lasted 420 s.

Stimulus presentation inside the scanner used a stereoscopic projector system. The right and left eye images were alternately displayed with a Christie Mirage S +2K projector (Christie Digital Systems, Cypress, CA) at 100 Hz (1,400 × 1,050 pixels) and quad-buffered with OpenGL stereo support (Quadro FX 1400; Nvidia, Santa Clara, CA). A ZScreen (RealD StereoGraphics, Mission Viejo, CA) differentially polarized images of the right and left eyes at a frequency that was temporally synchronized with the refresh rate of the projector. Light polarization was circular to eliminate the introduction of cross talk between the left and right eyes by small misalignments of the head. Stimuli were displayed at the back of the scanner bore on a projection screen (ST-Professional-DC, Screen-Tech, Hamburg, Germany) that preserved the polarization of the projected beams and were viewed with matching polarized eyewear through a mirror attached to the head coil. The visual field had a diameter of about 26°.

Subjects were instructed to fixate the central cross and to indicate, by a button press, which sinusoid had the greater amplitude. Stimulus presentation was controlled by custom-made software and followed a block design, with the method of constant stimuli and a two-alternative forced-choice task. Each run comprised three 14-trial blocks for each of the five conditions (four pedestal disparities and the baseline) that were interleaved pseudorandomly. In the four pedestal conditions,

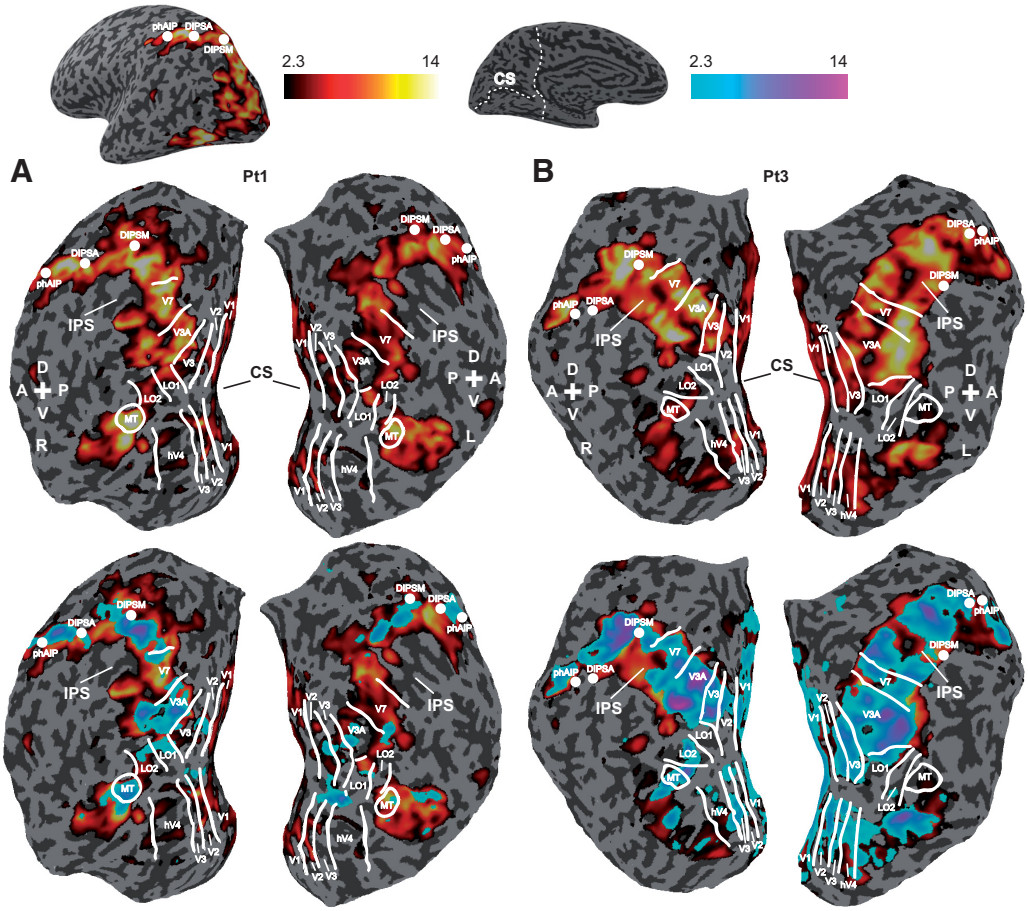

FIG. 2. Significant blood oxygenation level dependent (BOLD) activity to pedestal disparities of 0° and 0.7° shown on the flattened brains of subjects 1 (*A*) and 3 (*B*). *Top row*: the data for the 0.7° pedestal with a "hot" colormap (shades of red and yellow), whereas the bottom row shows the same data but with the activation to the 0° pedestal superimposed on the 0.7° data with a "cool" color map (shades of blue and purple). The *z*-statistic for the significant activation ranges from 2.3 to 14. The images illustrate the boundaries of retinotopically mapped areas and the center-of-gravity (COG) of the 3 intraparietal regions dorsal intraparietal sulcus anterior (DIPSA), dorsal intraparietal sulcus medial (DIPSM), and putative human anterior intraparietal (phAIP). R and L indicate the right and left hemispheres, whereas CS and IPS mark the locations of the calcarine and intraparietal sulci, respectively. Anatomical directions are also labeled (D, dorsal; V, ventral; A, anterior; P, posterior). The inflated hemisphere (*top middle*) shows an example of how the inflated cortical surface was cut to produce a flat map. The cuts are shown in white and were made by cutting along the CS (labeled) and around the occipito-temporo-parietal region from medial to lateral. The flat maps can show minor variations depending on anatomical differences. *Inset*: representative rendering of an inflated hemisphere (subject 1) illustrating the COG of DIPSA, DIPSM, and phAIP with the activity to the 0.7° in the background.

every 14-trial block included two repetitions of each of the seven Δx values. Therefore at the end of testing, subjects viewed each possible amplitude of the sinusoid a total of 60 times, which resulted in 420 presentations at each pedestal disparity. The baseline condition contained only zero disparity and thus the same flat plane stimuli were presented throughout these blocks. To avoid interruptions of the task that could have introduced errors or response delays, subjects were instructed to respond randomly during these trials.

An individual trial lasted 2,000 ms, comprising a 300-ms stimulus presentation followed by 1,500 ms for the response and a 200-ms intertrial interval. A gray uniform field with the central fixation cross was presented after stimulus offset.

Three subjects were further tested in a control session designed to measure the response to the zero disparity baseline relative to fixation. This consisted of five runs with stimuli as described for the main experiment with the addition of three 14-trial blocks with the fixation-only stimulus. Thus each control run included six conditions (four pedestal disparities, baseline, and fixation-only) and resulted in a total of 252 trials. The behavioral task was as described for the main experiment, except that no response was required in the fixation-only condition.

Finally, two subjects were also tested in a second control session designed to measure the effect of differences in the uncorrelated dots distributions across the four pedestals. Each of these sessions included five runs that comprised the four conditions in the uncorrelated control stimulus set, the baseline stimuli, and the fixation-only condition, resulting in a total of 252 trials. The rest of the procedure was as described earlier.

Prior to testing in the scanner, subjects were trained in the psychophysical tasks with a red/green anaglyph system until they reached 75% correct criterion performance at all disparities.

Each functional session also included a T1-weighted image (3D FLASH) that was used to register the functional data to the whole brain anatomy. These slices were acquired coronally with a reduced field of view (FOV: 40 2-mm slices) and had an in-plane resolution of 1×1 mm^2.

Functional data analysis

BOLD signal analysis was carried out with the statistical software library FSL (v. 4.1.0, //www.fmrib.ox.ac.uk/fsl) and began with separate analyses for individual sessions for individual subjects. Statistical preprocessing comprised motion correction performed with MCFLIRT (Jenkinson and Smith 2001), spatial smoothing with a Gaussian kernel of full-width half-maximum of 5 mm, and nonlinear Gaussian-weighted high-pass temporal filtering. The first-level statistical analysis was performed with FILM (Woolrich et al. 2001) and included prewhitening to remove temporal autocorrelation. For the main analysis, the resulting z-statistic images contained significant cortical activity in the four disparity pedestals relative to the zero disparity baseline. For the analysis of the BOLD response in the scans with the fixation-only stimuli, the z-statistic images contained significant activity in the four disparity pedestals and in the baseline condition relative to fixation.

These data were further analyzed within subjects with a fixed-effects analysis to identify clusters of significant activation across the 10 runs. The registration of the 10 functional images to the corresponding anatomy was carried out with FLIRT (Jenkinson and Smith 2001). The images for the first-level and fixed-effects analyses were thresholded at $z > 2.3$ and used a significance level of $P < 0.05$ (corrected for multiple comparisons). The mean percentage BOLD change in the retinotopically defined visual areas and in the parietal areas was computed using the Featquery tool in FSL. Specifically, the activity to the condition of interest relative to the baseline was averaged across the voxels within the region considered and converted to percentage signal change.

The same method was used to analyze the data from the two control conditions, except that the fixed-effects analysis was carried out across five runs for each subject and that the resulting activity was relative to fixation.

Post hoc comparisons were carried out with repeated-measures t-tests, whereas significant activation above zero was assessed with a one-sample t-test. All t-tests were two-tailed and used significance levels adjusted with the Bonferroni correction.

Anatomical data collection and analysis

High-resolution, whole-brain T1-weighted images (3D FLASH) were acquired axially with a spatial resolution of $1 \times 1 \times 1$ mm. White/gray matter segmentation was performed with a semiautomated procedure (SurfRelax; Larsson 2001). This software was also used to inflate and flatten the resulting gray matter maps that provided a high-resolution space on which the functional data were overlaid.

Retinotopy

Retinotopic data were acquired coronally in a separate session with an EPI sequence (TE = 30 ms; TR = 4,000 ms; 40 2-mm slices; 2×2 mm in-plane resolution; matrix = 64×64). Each run consisted of 48 volumes acquired continuously (192 s). To identify not only human V5/MT, but also other retinotopically defined areas, the mapping stimulus was a wedge consisting of 500 black dots on a white background. The apex of the wedge was at the fixation point. This wedge subtended 90° and rotated 45° every TR (4 s). The dots within the wedge moved along radial trajectories inward and outward, changing direction every 1 s, as described in Bridge and Parker (2007). Each run consisted of six complete cycles of the wedge. The stimuli were displayed with a VSG 2/5 graphics card (Cambridge Research Systems, Cambridge, UK) and an XGA LCD projector on a rear-projection screen at the back of the scanner and viewed through a mirror attached to the head coil.

For two subjects, polar angle maps were obtained using retinotopic mapping stimuli that consisted of a contrast reversing (8 Hz) black and white checkerboard wedge (for experimental methods see Bridge and Parker 2007). The wedge subtended 45° and rotated through 30° every TR (4 s). The details of this EPI sequence were as described earlier, except that they included 72 volumes (288 s).

Each functional session also included a reduced FOV (40 2-mm slices) T1-weighted image (3D FLASH), acquired coronally at an in-plane resolution of 1×1 mm^2. These slices were in the same planes as the functional images and were used as an intermediate step to register the retinotopy data to the whole brain anatomy.

Polar angle maps were extracted with the mrVista package (http://white.stanford.edu/newlm/index.php/Software). This software was also used for motion correction and registration of the functional images to the anatomy. The resulting maps were displayed on flat renderings of the occipito-temporo-parietal region on which the borders between the visual areas were identified. Visual areas were transformed into three-dimensional space with custom-made software and their coordinates used to quantify the percentage BOLD signal change in the different conditions with Featquery.

Definitions of DIPSA, DIPSM, and phAIP

We also measured the cortical response of intraparietal sulcus (IPS) areas dorsal IPS anterior (DIPSA), dorsal IPS medial (DIPSM), and putative human anterior intraparietal region (phAIP). Along the IPS, DIPSM is the most posterior of these regions, phAIP is the most anterior, and DIPSA is located between the two. With respect to homologies with the monkey brain, DISPM has been suggested to correspond to anterior LIP, and DIPSA and phAIP to posterior and anterior AIP, respectively (Orban et al. 2006).

DIPSA, DIPSM, and phAIP were constructed around the MNI (Montreal Neurological Institute) coordinates (Mazziotta et al. 1995, 2001) of the center-of-gravity (COG) reported in Table 2 in Georgieva et al. (2009). A spherical region of interest (ROI) with a radius of 4 mm was constructed around these COGs in MNI space and then transformed into the high-resolution space of individual subjects. The percentage BOLD change in these structural ROIs was quantified as for the retinotopically mapped regions.

Psychophysical data analysis

Stereoacuity thresholds at each pedestal were processed in MATLAB (TheMathWorks, Natick, MA) with custom-made software and Probit analysis (Finney 1971). A cumulative Gaussian function was fitted to the proportion of correct responses (60 trials in total at each disparity tested) to estimate the disparity (Δx) corresponding to 75% correct discrimination for each stimulus configuration. Data from trials with crossed and uncrossed disparities were combined.

RESULTS

Significant BOLD activation was found throughout the visual cortex and into parietal areas for all the pedestal disparities in comparison with the activity due to the zero disparity, planar baseline stimulus. Figure 2 shows this cortical activation for the data at the 0.7° and the 0° pedestal disparity conditions for the two subjects with the best psychophysical performance. The activity is rendered on flattened brains and the 0.7° and 0° pedestal disparities are represented with the hot and cool color maps, respectively. The activations of the two remaining subjects are shown in Supplemental Fig. S1 (available at http://jn.physiology.org/ as supplemental material).[1]

[1] The online version of this article contains supplemental data.

Activation of retinotopic visual areas

To investigate further the effect of changing pedestal disparity on the cortical activation, we calculated the percentage BOLD change in retinotopically mapped visual areas. The signal changes in each area can be seen in Fig. 3*A*. In almost all cases, there is an increase in BOLD activity as the pedestal size is increased. This pattern is most evident in areas V7, MT, DIPSA, and DIPSM. The early visual areas show very little activity to the zero pedestal condition, whereas the response to this stimulus is robust in the dorsal areas, DIPSM and LO1. Differences between the visual areas were confirmed by a repeated-measures ANOVA, which yielded significant main effects of visual area [$F(8,312) = 16.055$; $P < 0.001$] and disparity [$F(3,117) = 12.139$; $P < 0.001$]. A significant interaction [$F(24,936) = 3.892$; $P < 0.001$] was also evident, which reflects the fact that the response in some visual areas (V1, V2, hV4, LO2, V7, and MT) increased steadily with pedestal disparity. LO1 responded equally strongly to the 0° and 0.1° conditions, whereas other areas reached saturation at the 0.35° pedestal.

To compare directly the response in the two visual streams, the data were combined into early (V1, V2, and V3), ventrolateral (hV4, LO1, and LO2), and dorsal (V3A, V7, and MT) clusters (Fig. 3*B*). As expected from the activity in individual areas, this combined response was significant at all pedestal values in dorsal and ventrolateral regions ($P < 0.005$) but only at the two larger nonzero pedestals in early visual cortex. Additionally, as indicated by a significant interaction in the repeated-measures ANOVA [$F(6,234) = 4.624$, $P < 0.005$], activity in the dorsal cluster was significantly greater at all the nonzero pedestal disparities compared with that at the zero disparity pedestal ($P < 0.003$). Such a difference was found for only the two larger pedestals for the early regions and for none

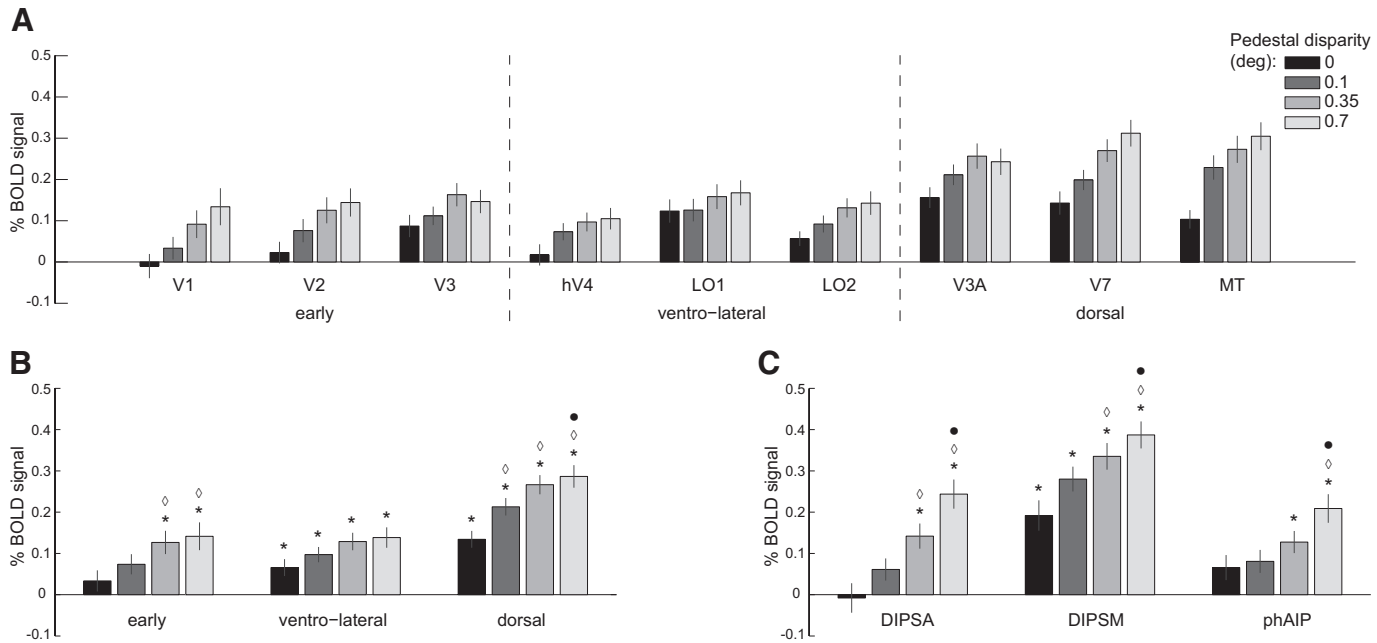

FIG. 3. *A*: mean blood oxygenation level dependent (BOLD) activity for individual areas to the 4 disparity pedestals. *B*: mean BOLD activity averaged for early, ventrolateral, and dorsal regions. *C*: mean BOLD activity for parietal regions DIPSA, DIPSM, and phAIP. The asterisk (*) indicates statistically significant activity relative to baseline, ◊ indicates statistically significant comparisons with the zero pedestal, and ● indicates statistically significant comparisons between the 0.1 and 0.7° pedestals. Error bars show the SE derived from combining all scans across subjects.

of the pedestals in ventrolateral cortex. Dorsal regions also responded more strongly to the 0.7° than to the 0.1° pedestal.

Parietal activation

In addition to the increase in response as a function of pedestal disparity in retinotopically mapped areas, Fig. 2 shows a cluster of regions with significant activity in parietal cortex, particularly the intraparietal sulcus. To investigate the disparity-related signals in this region, we quantified BOLD activity in areas DIPSA, DIPSM, and phAIP, defined anatomically as described in METHODS. As shown in Fig. 3*C*, the responses of these regions differed. The response in area DIPSM was the strongest. Activity in this region was significant at all values of pedestal ($P < 0.005$) and was greater for the two larger nonzero pedestals than that for the zero pedestal disparity ($P < 0.003$). Interestingly, unlike DIPSM and the dorsal visual areas, neither DIPSA nor phAIP showed much activity at the 0° pedestal, although the activation increased significantly with increasing pedestal. Note that the distance between V7 and DIPSM appears deceptively large for Pt1 in Fig. 2. Investigation showed that this is due to distortions created by the flattening algorithm.

Response to zero disparity stimuli

The baseline stimulus in the main experiment, a zero disparity plane, was designed to separate responses to disparity from those to the dots alone. However, this baseline stimulus will artifactually reduce the responses of visual areas with large populations of cells tuned for zero disparity. To ensure that this was not a major confound in our experiment, on three of the four subjects we performed an additional scanning session in which a fixation-only condition with no dots was used as a baseline.

Figure 4*A* shows the activation to the four pedestal conditions and to the zero disparity stimulus relative to the fixation-only condition in individual areas. The greatest response to the zero disparity stimulus is in the early visual areas, particularly V1, rather than in ventrolateral or dorsal visual areas. The response to the flat plane is essentially absent in all parietal regions (Fig. 4*C*). When the areas are clustered into early, ventrolateral, and dorsal regions (Fig. 4*B*), the weaker response in the ventrolateral and dorsal regions is evident. However, the relative response to the large pedestal disparities is greater in the dorsal and parietal areas compared with that in the early and ventrolateral areas.

Controlling for the level of uncorrelated dots

A further possible confound in the experiment is the distribution of uncorrelated dots in the stimulus. When horizontal disparity is added to a stimulus there will be a "hole" from where the dots have been moved. To prevent such a monocular cue appearing in the stimulus, uncorrelated dots were added to fill in this "hole." The different pedestal disparity stimuli, however, require different proportions of uncorrelated dots, which could theoretically drive the fMRI response. To rule out this possibility, we ran two subjects on a similar paradigm to the main experiment but with the uncorrelated dots added without a pedestal disparity. Analysis of the activation in the four pedestals with the "uncorrelated" stimuli shows no consistent effect of uncorrelated dots in any area (Supplemental Fig. S2).

Stereoacuity thresholds

It is well established that disparity discrimination thresholds increase with pedestal disparity. The psychophysical thresholds and corresponding behavioral performance in the four conditions for the group and the individual data are shown in Fig. 5. In agreement with previous psychophysical reports (Schumer and Julesz 1984), the discrimination thresholds for determining which of the two sinusoidal modulations had the

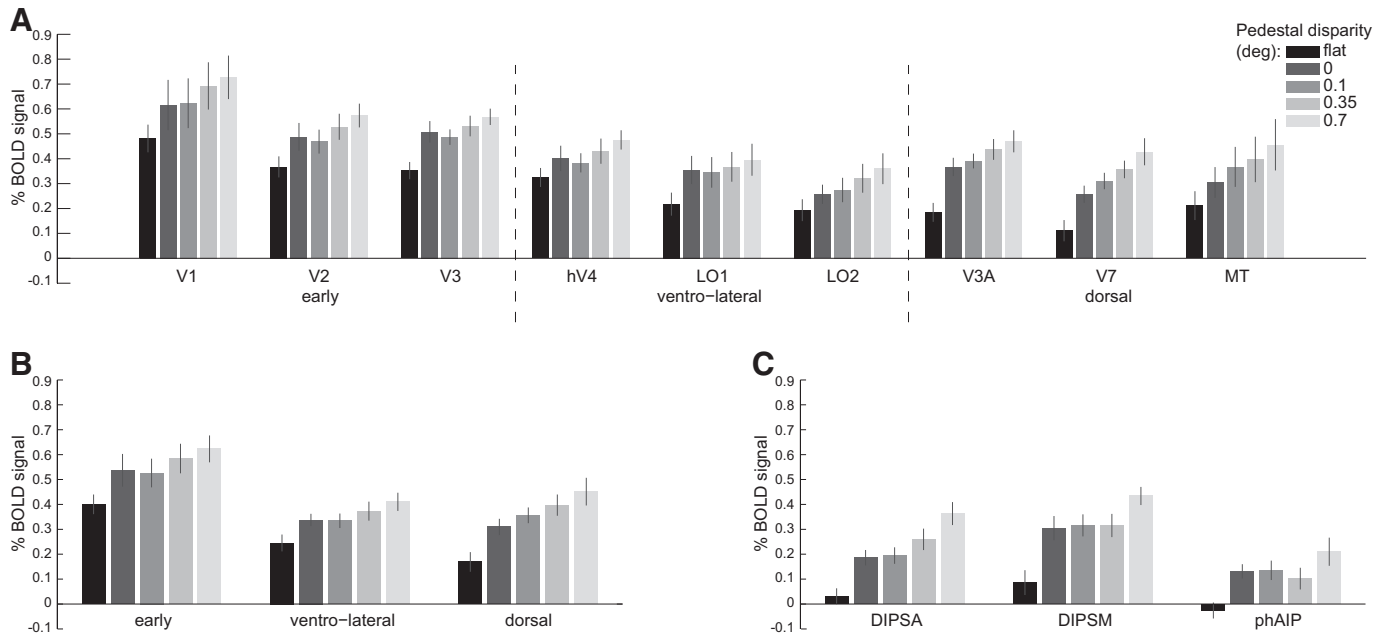

FIG. 4. *A*: mean BOLD activity for individual areas to the 4 disparity pedestals and baseline relative to fixation. *B*: mean BOLD activity averaged for early, ventrolateral, and dorsal regions. *C*: mean BOLD activity for parietal regions DIPSA, DIPSM, and phAIP.

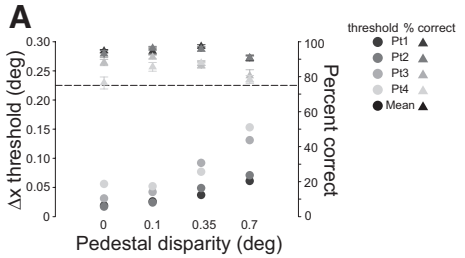

FIG. 5. Psychophysical thresholds for subjects to determine which of the 2 sinusoidal disparity modulations had the greater amplitude and corresponding behavioral performance in the 4 pedestals. The data are shown for individual subjects (*A*) and for the group (*B*). The dashed line marks criterion performance and error bars show SE across scans for each individual subject (*A*) and across pooled data for each subject (*B*).

greater amplitude increased with pedestal disparity for all four subjects. We observed greater variability in the thresholds at the largest pedestal, which was also reflected in poorer behavioral performance. Nevertheless, correct discrimination was relatively stable and above criterion (75% correct).

Relationship between BOLD and psychophysical responses

To quantify the relationship between cortical activity and behavioral performance, a comparison between the BOLD signal from trials with correct and incorrect responses was performed. Single-trial responses were extracted from postprocessed data (as described in METHODS) and analyzed using an event-related technique with the zero disparity flat plane as the baseline condition. Within each pedestal, the activity from trials in which Δx was 0 (i.e., trials for which there was no correct response because the amplitude of the two sinusoids was the same) was computed separately, but it was not used in this analysis.

The comparison of the correct and incorrect trials for each of the retinotopic visual areas is shown in Fig. 6 (*top row*), indicating a greater BOLD response to the correct relative to the incorrect trials in most conditions. A repeated-measures ANOVA was performed with area (the nine retinotopically defined areas), pedestal (0, 0.1, 0.35, and 0.7°), and performance (correct and incorrect) as within-subjects factors. Significant main effects of area [$F(8,312) = 13.094$, $P < 0.001$], pedestal [$F(3,117) = 3.250$, $P < 0.05$], and performance [$F(1,39) = 7.778$, $P < 0.01$] were found. When the data were binned across the early, ventrolateral, and dorsal areas (Fig. 6, *middle row*), only the dorsal region showed a significantly greater response to correct than to incorrect trials and only at the largest pedestal (0.7°). The latter results were significant on post hoc two-tailed *t*-tests comparing correct and incorrect trials designed to explore the significant interactions of cluster × pedestal [$F(6,234) = 3.697$, $P < 0.01$] and cluster × performance [$F(2,78) = 5.472$, $P < 0.01$].

In the three parietal regions a significantly greater cortical response for correct trials was found in DIPSA and DIPSM, again at the 0.7° pedestal ($P < 0.001$). For both the dorsal and DIPSM regions, the comparisons between correct and incorrect

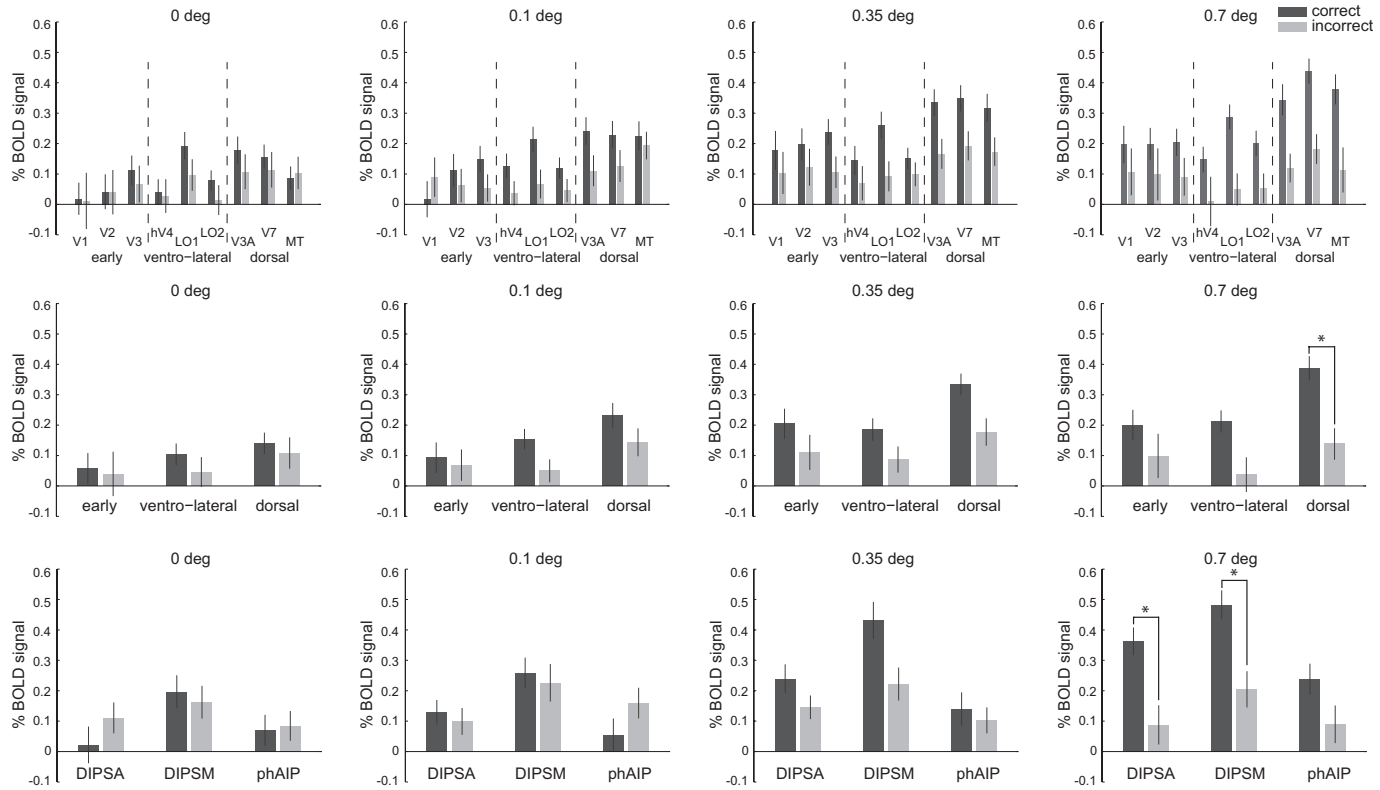

FIG. 6. BOLD response on correct and incorrect trials in individual (*top row*) and clustered (*middle row*) retinotopically mapped areas and in the 3 parietal regions (*bottom row*). Asterisks (*) indicate significant contrasts between cortical activation in correct and incorrect trials. Error bars show the SE derived from combining all scans across subjects.

responses at the 0.35° pedestal narrowly missed significance after correction. These data are shown in the *bottom row* of Fig. 6.

DISCUSSION

Widespread cortical activity was generated throughout the occipitoparietal regions by stimuli modulated in depth defined by binocular disparity. Comparisons between early, ventrolateral, and dorsal retinotopic visual areas indicated that, although all regions showed some increase in response with pedestal disparity, the dorsal system is modulated most by the increases of disparity magnitude. Parietal regions showed a similar pattern of response as a function of disparity to dorsal areas. The data also indicate that in both these regions the BOLD activation is significantly greater in correct compared with that in incorrect trials, most notably at large pedestal disparities.

Dorsal visual pathway encodes a larger disparity range

When a pedestal disparity is added to the stimulus, this locates the modulations in depth further away from the fixation plane. This results in an increase in activation in the dorsal visual areas. For all three nonzero pedestals, the activation is significantly greater than that due to the zero pedestal, although, with the exception between the 0.1° and 0.7° conditions, it does not differ between the three nonzero pedestals. By contrast, this difference was observed for only the two larger pedestals in early visual cortex and for none of the pedestals in ventrolateral regions. In these latter areas, the activation showed no significant differences among any of the pedestal conditions.

All stimuli that we presented included a range of disparities within the stimulus, due to the sinusoidal modulation of disparity, which is present even in those stimuli with zero pedestal disparity. The addition of the pedestal disparity increases the total depth range in the person's visual field. At a neuronal level, there are at least two possible explanations of the response of dorsal areas. First, it may be that some of the disparity-tuned neurons in these regions are simply more coarsely tuned and therefore respond to all the pedestals, whereas those in the other regions respond less well to the largest disparities. Second, the population of neurons may cover a greater range of selectivities such that, at the larger pedestals, additional disparity-selective neurons are recruited.

The ventrolateral areas are generally considered to be involved in detailed vision such as object, shape, and face recognition (for review, see Grill-Spector and Malach 2004). Therefore it is less likely that very large disparities would be useful for these tasks. Furthermore, to accurately perceive these objects, subjects will converge in the most appropriate depth plane and therefore reduce the range of disparities necessary for perception. For these reasons, it may be appropriate for ventrolateral regions to display less responsiveness to large pedestal disparities. The small effect of disparity magnitude that we obtained in this study is consistent with Preston et al. (2008) who showed, using a completely different paradigm, that LO is modulated by the "sign" of the disparity (i.e., near or far), but not by its magnitude.

Our finding that the dorsal visual regions respond to a greater range of disparities than that of the early visual cortex has implications for how disparity information is processed in visual cortex. A plausible view is that disparity sensitivities in extrastriate cortex result from subsampling the range of distributions in early visual cortex, in particular V1. Subsampling could generate new properties in the extrastriate disparity distribution, but it is unlikely that this process could increase the disparity range. Our results could be accounted for if binocular neurons in extrastriate cortex compute the signal *1*) from monocular neurons in V1 or *2*) from a pathway that bypasses V1. Although at present speculative, these are testable predictions that should be addressed in future studies.

Parietal regions differ in their response patterns

The parietal regions clearly show considerable activation to these disparity defined depth stimuli. To investigate any differences occurring along the IPS, we applied the terminology of Georgieva et al. (2009) who subdivided the region to include areas DIPSM, DIPSA, and phAIP. In the current study, the response of DIPSM is very similar to the dorsal visual areas, whereas DIPSA and phAIP show little response to the zero disparity pedestal condition, but increasing responses to the larger pedestals. This difference is consistent with the definitions of Georgieva et al. (2009) because LIP (DIPSM homologue) is more closely related to the dorsal visual stream, involved in saccades and decision making (Schluppeck et al. 2005, 2006; Sereno et al. 2001; Silver et al. 2005), whereas AIP (DIPSA and phAIP homologue) is more involved in reaching and grasping (tasks that may on occasion be supported by large differences in stereo disparity; Tunik et al. 2005).

Psychophysical task directs attention to the stimuli

Although the importance of controlling attention using psychophysical tasks is widely accepted, there are detailed differences in paradigms that affect the extent to which the task is related to the stimulus dimension under experimental study, depth in this case. The current experiment was designed to meet this goal, so that the observer performed a task that required discrimination of the amplitude of depth modulation. Furthermore, the experimental conditions were such that performance, measured by percentage correct responses, was matched as closely as possible across different values of disparity pedestal. All subjects were performing at this criterion (75% correct) outside the scanner prior to commencing the scanning sessions.

A previous study has shown that BOLD activity in depth tasks is correlated with task performance in area MT+ and LO regions (Chandrasekaran et al. 2007). However, in their experiment the performance was determined for a range of difficulty levels for the task. In the current experiment, such a parametric variation was not used and therefore the distribution of correct responses was narrow. Under our circumstances, a more useful measure of the effect of performance on BOLD activation was the direct comparison of correct and incorrect trials.

In both dorsal areas and parietal areas DIPSA and DIPSM, there is a significant decrease in the activation to incorrect compared with correct trials at the largest pedestal. The psychophysical response does not affect levels of activation at the smaller disparity pedestals in any regions. Furthermore, there are no significant differences between the correct and incorrect trials in the early, ventrolateral, and phAIP regions.

The reduction in activation for incorrect trials suggests that reduced cortical response in certain brain regions is associated with poorer performance in stereoscopic depth tasks.

Receptive field profiles could influence differences between visual regions

A difference in the receptive field properties in disparity-selective neurons across visual areas could also underlie the present observations. Cumming and DeAngelis (2001) point out that, in the macaque monkey, there appears to be a systematic shift in disparity-selective neurons from even symmetric in V1 to odd symmetric in V5/MT and MST. If this were also generally the case in the human dorsal visual areas, the prediction is that there would be larger responses to disparities that are at a considerable distance from the fixation plane, such as those with large pedestal disparities.

A further consideration related to receptive field profiles is that the baseline condition in this experiment was a zero disparity flat plane that was presented for 300 ms of each 2 s trial just like the other conditions. This stimulus was designed to identify any components of the response that were related to the presence of the dots rather than depth information, while allowing subjects to maintain fusion. However, this stimulus is also an optimal stimulus for disparity-selective cells tuned for zero disparity. Neurophysiologically, V1 has an abundance of neurons tuned for zero disparity (Poggio and Fischer 1977; Poggio et al. 1988; Prince et al. 2002). Analyses of the activation to the baseline condition and pedestal disparities relative to fixation suggest that the relatively small response in the early visual areas compared with the dorsal (and to a certain extent the ventrolateral regions, particularly hV4) does not reflect a relatively large activation in the baseline condition. The response rate to all stimuli compared with fixation, however, is considerably larger in the early visual areas.

The data from the second control condition clearly rule out the possibility that the different proportion of uncorrelated dots in the pedestal conditions could have acted as a confounding variable. No significant interaction was found that could account for our main results.

Vergence eye movements do not help

We did not monitor the vergence eye movements of our subjects. However, the stimuli were of short duration (300 ms) to reduce the potential for convergence or divergence. The task was challenging even with these stimulus durations, so reducing the presentation time to 100 ms would have made it almost impossible to perform adequately across all conditions. However, two additional properties of the experimental design make vergence unlikely as an explanation of the results. First, the pedestal disparity is added in opposite directions in the two hemifields, such that there is no net drive for convergence to a particular disparity plane. Second, converging on one of the stimuli is not useful because the subjects were required to compare the modulation depth between the two stimuli.

Conclusion

We have shown that adding a pedestal disparity to a depth discrimination task increases activity most significantly in dorsal visual areas and parietal areas. These results suggest that the dorsal visual system, both occipital and parietal, may provide greater depth discrimination at large disparities.

ACKNOWLEDGMENTS

We thank D. Schluppeck for helpful comments, M. Zannoli for pilot data acquisition, and S. Knight for radiographer assistance.

GRANTS

This research was supported by the Medical Research Council (United Kingdom). H. Bridge is a Royal Society University Research Fellow and A. Parker holds a Wolfson Research Merit Award from the Royal Society.

DISCLOSURES

No conflicts of interest, financial or otherwise, are declared by the author(s).

REFERENCES

Backus BT, Fleet DJ, Parker AJ, Heeger DJ. Human cortical activity correlates with stereoscopic depth perception. *J Neurophysiol* 86: 2054–2068, 2001.

Bradley DC, Chang GC, Andersen RA. Encoding of three-dimensional structure-from-motion by primate area MT neurons. *Nature* 392: 714–717, 1998.

Bridge H, Parker AJ. Topographical representation of binocular depth in the human visual cortex using fMRI. *J Vis* 7: Article 15 (11–14), 2007.

Chandrasekaran C, Canon V, Dahmen JC, Kourtzi Z, Welchman AE. Neural correlates of disparity-defined shape discrimination in the human brain. *J Neurophysiol* 97: 1553–1565, 2007.

Cumming BG, DeAngelis GC. The physiology of stereopsis. *Annu Rev Neurosci* 24: 203–238, 2001.

Cumming BG, Parker AJ. Responses of primary visual cortical neurons to binocular disparity without depth perception. *Nature* 389: 280–283, 1997.

Cumming BG, Parker AJ. Binocular neurons in V1 of awake monkeys are selective for absolute, not relative, disparity. *J Neurosci* 19: 5602–5618, 1999.

Cumming BG, Parker AJ. Local disparity not perceived depth is signaled by binocular neurons in cortical area V1 of the macaque. *J Neurosci* 20: 4758–4767, 2000.

Dodd JV, Krug K, Cumming BG, Parker AJ. Perceptually bistable three-dimensional figures evoke high choice probabilities in cortical area MT. *J Neurosci* 21: 4809–4821, 2001.

Finney DJ. *Probit Analysis.* London: Cambridge Univ. Press, 1971.

Georgieva S, Peeters R, Kolster H, Todd JT, Orban GA. The processing of three-dimensional shape from disparity in the human brain. *J Neurosci* 29: 727–742, 2009.

Grill-Spector K, Malach R. The human visual cortex. *Annu Rev Neurosci* 27: 649–677, 2004.

Janssen P, Vogels R, Liu Y, Orban GA. At least at the level of inferior temporal cortex, the stereo correspondence problem is solved. *Neuron* 37: 693–701, 2003.

Janssen P, Vogels R, Orban GA. Macaque inferior temporal neurons are selective for disparity-defined three-dimensional shapes. *Proc Natl Acad Sci USA* 96: 8217–8222, 1999.

Jenkinson M, Smith S. A global optimisation method for robust affine registration of brain images. *Med Image Anal* 5: 143–156, 2001.

Krug K, Cumming BG, Parker AJ. Comparing perceptual signals of single V5/MT neurons in two binocular depth tasks. *J Neurophysiol* 92: 1586–1596, 2004.

Larsson J. *Imaging Vision: Functional Mapping of Intermediate Visual Processes in Man* (PhD Thesis). Stockholm: Karolinska Institute, 2001.

Mazziotta J, Toga A, Evans A, Fox P, Lancaster J, Zilles K, Woods R, Paus T, Simpson G, Pike B, Holmes C, Collins L, Thompson P, MacDonald D, Iacoboni M, Schormann T, Amunts K, Palomero-Gallagher N, Geyer S, Parsons L, Narr K, Kabani N, Le Goualher G, Boomsma D, Cannon T, Kawashima R, Mazoyer B. A probabilistic atlas and reference system for the human brain: International Consortium for Brain Mapping (ICBM). *Philos Trans R Soc Lond B Biol Sci* 356: 1293–1322, 2001.

Mazziotta JC, Toga AW, Evans A, Fox P, Lancaster J. A probabilistic atlas of the human brain: theory and rationale for its development. The Interna-

tional Consortium for Brain Mapping (ICBM). *NeuroImage* 2: 89–101, 1995.

Neri P. A stereoscopic look at visual cortex. *J Neurophysiol* 93: 1823–1826, 2005.

Neri P, Bridge H, Heeger DJ. Stereoscopic processing of absolute and relative disparity in human visual cortex. *J Neurophysiol* 92: 1880–1891, 2004.

Orban GA, Claeys K, Nelissen K, Smans R, Sunaert S, Todd JT, Wardak C, Durand JB, Vanduffel W. Mapping the parietal cortex of human and non-human primates. *Neuropsychologia* 44: 2647–2667, 2006.

Parker AJ. Binocular depth perception and the cerebral cortex. *Nat Rev Neurosci* 8: 379–391, 2007.

Poggio GF, Fischer B. Binocular interaction and depth sensitivity in striate and prestriate cortex of behaving rhesus monkey. *J Neurophysiol* 40: 1392–1405, 1977.

Poggio GF, Gonzalez F, Krause F. Stereoscopic mechanisms in monkey visual cortex: binocular correlation and disparity selectivity. *J Neurosci* 8: 4531–4550, 1988.

Preston TJ, Li S, Kourtzi Z, Welchman AE. Multivoxel pattern selectivity for perceptually relevant binocular disparities in the human brain. *J Neurosci* 28: 11315–11327, 2008.

Prince SJ, Cumming BG, Parker AJ. Range and mechanism of encoding of horizontal disparity in macaque V1. *J Neurophysiol* 87: 209–221, 2002.

Schluppeck D, Curtis CE, Glimcher PW, Heeger DJ. Sustained activity in topographic areas of human posterior parietal cortex during memory-guided saccades. *J Neurosci* 26: 5098–5108, 2006.

Schluppeck D, Glimcher P, Heeger DJ. Topographic organization for delayed saccades in human posterior parietal cortex. *J Neurophysiol* 94: 1372–1384, 2005.

Schumer RA, Julesz B. Binocular disparity modulation sensitivity to disparities offset from the plane of fixation. *Vision Res* 24: 533–542, 1984.

Sereno MI, Pitzalis S, Martinez A. Mapping of contralateral space in retinotopic coordinates by a parietal cortical area in humans. *Science* 294: 1350–1354, 2001.

Silver MA, Ress D, Heeger DJ. Topographic maps of visual spatial attention in human parietal cortex. *J Neurophysiol* 94: 1358–1371, 2005.

Tanabe S, Umeda K, Fujita I. Rejection of false matches for binocular correspondence in macaque visual cortical area V4. *J Neurosci* 24: 8170–8180, 2004.

Tsao DY, Vanduffel W, Sasaki Y, Fize D, Knutsen TA, Mandeville JB, Wald LL, Dale AM, Rosen BR, Van Essen DC, Livingstone MS, Orban GA, Tootell RB. Stereopsis activates V3A and caudal intraparietal areas in macaques and humans. *Neuron* 39: 555–568, 2003.

Tunik E, Frey SH, Grafton ST. Virtual lesions of the anterior intraparietal area disrupt goal-dependent on-line adjustments of grasp. *Nat Neurosci* 8: 505–511, 2005.

Uka T, DeAngelis GC. Contribution of area MT to stereoscopic depth perception: choice-related response modulations reflect task strategy. *Neuron* 42: 297–310, 2004.

Uka T, DeAngelis GC. Linking neural representation to function in stereoscopic depth perception: roles of the middle temporal area in coarse versus fine disparity discrimination. *J Neurosci* 26: 6791–6802, 2006.

Umeda K, Tanabe S, Fujita I. Representation of stereoscopic depth based on relative disparity in macaque area V4. *J Neurophysiol* 98: 241–252, 2007.

Woolrich MW, Ripley BD, Brady M, Smith SM. Temporal autocorrelation in univariate linear modeling of FMRI data. *NeuroImage* 14: 1370–1386, 2001.